Localized Proton MRS of Cerebral Metabolite Profiles in Different Mouse Strains

Attila Schwarcz, Oliver Natt, Takashi Watanabe, Susann Boretius, Jens Frahm, and Thomas Michaelis*

Localized proton MR spectroscopy (MRS) was used to quantify cerebral metabolite concentrations in NMRI (n = 8), BALB/c (n = 7), and C57BL/6 (n = 8) mice in vivo and 1 hr after global irreversible ischemia (2.35 T, STEAM, TR/TE/TM = 6000/20/10 ms, 4 × 3 × 4 mm^3 volume, corrections for cerebrospinal fluid). Anatomical MRI and proton MRS revealed significant differences of the C57BL/6 strain in comparison with both BALB/c and NMRI mice. While MRI volumetry yielded larger ventricular spaces of the C57BL/6 strain, proton MRS resulted in elevated concentrations of *N*-acetylaspartate (tNAA), creatine and phosphocreatine (tCr), choline-containing compounds (Cho), glucose (Glc), and lactate (Lac) relative to BALB/c mice and elevated Glc relative to NMRI mice. Apart from the expected decrease of Glc and increase of Lac 1 hr post mortem, C57BL/6 mice presented with significant reductions of tNAA, tCr, and Cho, whereas these metabolites remained unchanged in BALB/c and NMRI mice. The results support the hypothesis that the more pronounced vulnerability of C57BL/6 mice to brain ischemia is linked to strain-dependent differences of the cerebral energy metabolism. Magn Reson Med 49:822–827, 2003.

Key words: magnetic resonance spectroscopy (MRS); mouse strain; brain metabolism; global cerebral ischemia

Advances in transgenic mouse technology enable investigations of specific molecular and cellular mechanisms underlying the pathophysiology of acute stroke (1,2). A putative problem of such studies emerges from the neurobiologic variability of transgenic mice that originate from different strains (3,4). For example, the frequently used C57BL/6 mice present with a much larger susceptibility to ischemic events than other strains (4–7). In this respect, the anatomic variability of the circle of Willis has been discussed as a major factor determining the sensitivity of mouse brain to stroke (8–11). However, further complications may arise from filament techniques commonly used to induce focal ischemia. This is because infarct volumes may differ when the gauge is not matched to the body weight, which varies among mouse strains at the same age (5,12).

To avoid hemodynamic variabilities caused by strain-related differences in anatomy and to rule out complications due to the induction of ischemia, the present work used localized proton MR spectroscopy (MRS) of cerebral metabolites in a model of irreversible global ischemia and in comparison with basal metabolite profiles obtained in vivo. The single-voxel MRS approach has previously been applied to quantify age- and gender-dependent concentrations of brain metabolites such as *N*-acetylaspartate (tNAA), creatine and phosphocreatine (tCr), choline-containing compounds (Cho), *myo*-inositol (Ins), glucose (Glc), and lactate (Lac) in humans and small mammals (see, for example, Refs. 13–15). So far, however, quantitative assessments of cerebral metabolite profiles in mouse strains in vivo are rare (3), as most studies were performed in vitro (16,17). Thus, the purpose of this study was 1) to determine the in vivo concentrations of brain metabolites in commonly used mouse strains, and 2) to investigate the metabolic responses to global irreversible ischemia in these strains.

MATERIALS AND METHODS

Animals and Anesthesia

All studies were performed in accordance with German animal protection laws after approval by the responsible governmental authority. Animals had free access to food and water. The investigated mice (male, 8–9 weeks old) from three different strains had mean body weights of 39 ± 5 g (NMRI, n = 8), 23 ± 1 g (BALB/c, n = 7), and 24 ± 2 g (C57BL/6, n = 8). Additional NMRI (n = 4), BALB/c (n = 3), and C57BL/6 (n = 3) mice were used in a preceding study evaluating two methods for a determination of cerebrospinal fluid (CSF) contributions to the volume-of-interest (VOI) selected for proton MRS.

Anesthesia was induced by i.p. injection of a mixture of xylazine (12.5 mg/kg), ketamine (125 mg/kg), and atropine (0.08 mg/kg). Animals were intubated with a polyethylene endotracheal tube and artificially ventilated. Anesthesia was maintained using 0.2–0.6% halothane in a 7:3 mixture of N_2O and O_2. For MRI/MRS animals were placed in a prone position on a custom-built palate holder equipped with an adjustable nose cone. The rectal temperature was maintained constant (37 ± 0.5°C) by heated water blankets positioned around the body. Irreversible global ischemia after cardiac arrest was induced by overdosing halothane, while heating of the body was continued.

Proton MRS

MR experiments were conducted at 2.35 T (MRBR 4.7/400 mm magnet, Magnex Scientific, Abingdon, England) with use of 100 mT/m gradients and a DBX system (Bruker Biospin, Ettlingen, Germany). Excitation and signal reception were accomplished with a Helmholtz coil (100 mm)

Biomedizinische NMR Forschungs GmbH am Max-Planck-Institut für biophysikalische Chemie, Göttingen, Germany.

Grant sponsors: DAAD; NKFP; Grant number: 1/A 00026/2002 (to A.S.).

A. Schwarcz's permanent address is Department of Neurosurgery, University of Pecs, Hungary.

*Correspondence to: T. Michaelis, Ph.D., Biomedizinische NMR Forschungs GmbH, 37070 Göttingen, Germany. E-mail: tmichae@gwdg.de

Received 25 November 2002; revised 19 December 2002; accepted 7 January 2003.

DOI 10.1002/mrm.10445
Published online in Wiley InterScience (www.interscience.wiley.com).

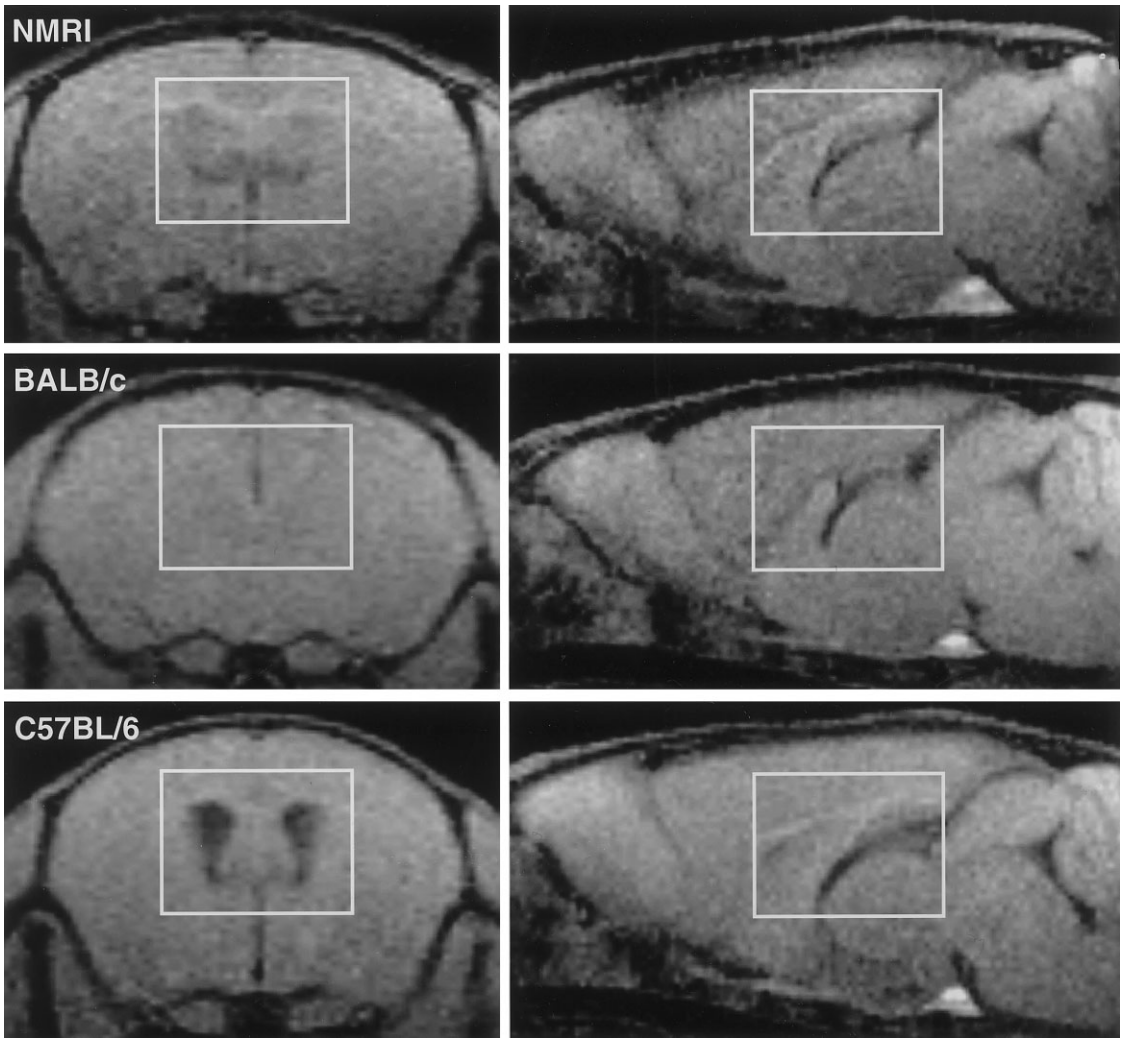

FIG. 1. T_1-weighted MRI (3D FLASH, TR/TE = 17/7.58 ms, flip angle 20°) of the brain of different mouse strains demonstrating the position of the VOI within (left) coronal and (right) midsagittal sections. The VOI was centrally placed within the forebrain using the pituitary gland as a boarder reference in the axial direction. The CSF contribution from the ventricular spaces is considerably smaller in NMRI and BALB/c mice than in the C57BL/6 strain.

and surface coil (16 mm), respectively. As demonstrated in Fig. 1, two sets of 3D gradient-echo images (spoiled FLASH, TR/TE = 17/7.58 ms, 20° flip angle) in coronal ($15 \times 20 \times 30$ mm^3 field of view, $128 \times 128 \times 64$ matrix) and sagittal orientation ($15 \times 15 \times 15$ mm^3 field of view, $128 \times 128 \times 32$ matrix) were obtained to assess strain-related differences in anatomy and to locate the VOI for proton MRS ($4 \times 3 \times 4$ mm^3) in a central position of the forebrain.

After localized shimming by FASTMAP (18), fully relaxed short-echo time proton MR spectra (STEAM, TR/TE/TM = 6000/20/10 ms, 64 accumulations, eight sequential recordings) were acquired in vivo as well as after cardiac arrest starting 4–5 min post mortem. The individual spectra were processed by LCModel (19) and combined into an in vivo and post mortem MR spectrum consisting of 8×64 accumulations each. Metabolite quantification with LCModel used the brain water signal as an internal reference assuming a mean tissue concentration of 43.7 mol/l reported for mouse brain (20–22). Statistical differences of in vivo metabolite concentrations between mouse strains were determined by an unpaired Student's *t*-test. A paired Student's *t*-test was performed for the assessment of statistically significant alterations between in vivo and post-mortem conditions within the same mouse strain.

CSF Partial Volume Correction

A first step attempted to validate MRI volumetry as a reliable method for estimating the CSF contribution by comparing it with the spectroscopic T_2 method which exploits a biexponential analysis of the T_2 relaxation decay of the brain water signal (23). MRI volumetry was based on coronal images using a free-hand delineation of the CSF spaces within the VOI. The sum of the identified areas was multiplied by the section thickness to calculate the CSF partial volume of the VOI. The molar quantity of the brain tissue water M_{Tissue} and its corresponding value M_{CSF} in CSF were obtained by assuming water concentrations of 43.7 mol/l and 55.6 mol/l (i.e., pure water), respec-

Table 1
MRS T_2 Analysis and MRI Volumetry of CSF Partial Volumes

	NMRI (n = 4)	BALB/c (n = 3)	C57BL/6 (n = 3)
$T_{2\text{-fast}}$	62 ± 4	62 ± 2	59 ± 2
$T_{2\text{-slow}}$	302 ± 109	282 ± 62	575 ± 117
MRS: f_{CSF}	2.7 ± 1.5	1.3 ± 0.5	9.5 ± 1.9
MRI: f_{CSF}	2.0 ± 1.1	1.5 ± 0.2	10.1 ± 1.5

The values represent mean ± SD averaged across animals. Relaxation times are given in ms, f_{CSF} = CSF partial volume fraction in percent of VOI.

tively. Using the CSF partial volume fraction $f_{CSF} = M_{CSF}/(M_{Tissue} + M_{CSF})$, the concentration $C_{LCModel}$ given by LCModel was corrected as follows:

$$C = C_{LCModel}/(1 - f_{CSF}). \quad [1]$$

Alternatively, the value for f_{CSF} was determined by acquiring fully relaxed proton MR spectra (STEAM, TR/TM = 6000/10 ms, 32 accumulations) of the unsuppressed water signal at echo times TE of 20, 30, 45, 68, 100, 150, 200, 275, 350, 425, 500, 625, 750, 875, 1000, 1250, and 1500 ms. The MR spectra were fitted to a biexponential decay function and the slow component was assumed to result from CSF. Accordingly, f_{CSF} corresponds to the signal amplitude of the slow component at TE = 0. A linear regression examined the correlation between the results obtained by MRI volumetry and MRS T_2 analysis.

RESULTS AND DISCUSSION

CSF Contributions and T_2 Relaxation

The mean results of the MRS T_2 analysis and MRI volumetry of brain tissue in NMRI, BALB/c, and C57BL/6 mice are summarized in Table 1. When plotting the CSF partial volume fractions f_{CSF} obtained for individual animals from volume determinations or the slow T_2 component as shown in Fig. 2, the two methods are in excellent agreement. A linear regression revealed a correlation coefficient of $r = 0.98$, a slope of 1.02, and an intercept close to zero. These findings suggest that MRS T_2 analysis and MRI volumetry provide equivalent estimates of the CSF partial volume fraction in brain tissue. Although volumetric evaluations may be time-consuming during postprocessing, the approach does not compromise the actual MRI/MRS experiment by additional acquisitions because suitable MRI data is available as an integral part of the MRS protocol. In contrast, a precise T_2 determination of the slow component requires a large number of additional MRS recordings at prolonged echo times where even the unsuppressed water resonance in a small VOI has a low SNR. Therefore, to keep the measuring time for in vivo MRS within reasonable limits, the CSF contributions in the main part of this study were determined by MRI volumetry.

The water proton T_2 relaxation time of about 60 ms for the fast "tissue" component in all mouse strains corresponds to a theoretical minimum linewidth of about 5 Hz at 2.35 T (FWHM, full width at half maximum). As shown in Table 2, this best resolution is not achievable because of residual intrinsic magnetic field inhomogeneities in brain tissue which most likely reflect structural susceptibility differences at a microscopic, i.e., cellular and subcellular, level. The observation that the spectral linewidth in mice brain is about 1.5-fold larger than that of comparable studies in rats is in agreement with findings by others (16). Surprisingly, however, with an in vivo FWHM of more than 9 Hz, the line broadening seems to be much more pronounced in the C57BL/6 strain than in NMRI and BALB/c mice, yielding only about 7 Hz. Potentially related to this phenomenon is the trend indicated in Table 1 and confirmed in Table 2 that C57BL/6 mice exhibit significantly larger CSF partial volume fractions by about a factor of 3 than both NMRI and BALB/c mice. Correspondingly enlarged ventricular spaces are appreciated by visual inspection of the T_1-weighted images shown in Fig. 1.

Cerebral Metabolite Profiles

Figure 3 compares in vivo and post mortem MR spectra of an NMRI, BALB/c, and C57BL/6 mouse. Similar to other mammals, the MR spectra reveal resonances of major cerebral metabolites such as tNAA, tCr, Cho, and Ins, as well as Glc and Lac. The resulting SNR turned out to be sufficient for a reliable spectral evaluation by LCModel and comparable to another proton MRS study of mice brain (24). Mean cerebral metabolite concentrations are summarized in Table 2. The most remarkable in vivo finding is the observation of a significantly different metabolite profile in the C57BL/6 strain in comparison with NMRI and BALB/c mice. In particular, C57BL/6 mice exhibit higher brain concentrations of tNAA, tCr, Cho, Glc, and Lac than BALB/c mice, as well as higher Glc levels than NMRI mice.

In general, the proton MRS-detected in vivo profiles of cerebral metabolites in NMRI, BALB/c, and C57BL/6 mouse strains are within the range of values reported for other mammal species in vivo (13–15) as well as for mice

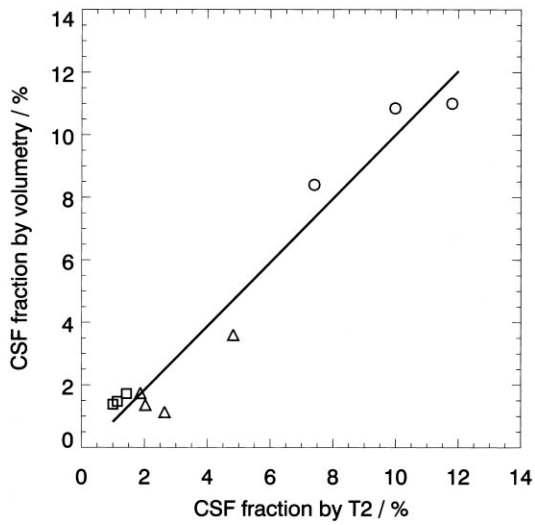

FIG. 2. Linear regression of the CSF partial volume fractions of NMRI (n = 4, triangles), BALB/c (n = 3, squares), and C57BL/6 mice (n = 3, circles) as determined by MRI volumetry and MRS T_2 measurements of the unsuppressed water signal within the VOI selected for MRS.

Table 2
MRS Parameters, CSF Partial Volumes, and Cerebral Metabolite Concentrations

	NMRI (n = 8)		BALB/c (n = 7)		C57BL/6 (n = 8)	
	In vivo	Post mortem	In vivo	Post mortem	In vivo	Post mortem
FWHM	7.6 ± 0.8**	9.4 ± 1.6†	6.9 ± 0.6***	7.8 ± 0.8	9.3 ± 1.0	8.6 ± 0.8
SNR	7.1 ± 2.0	6.5 ± 1.4	7.6 ± 0.8	7.3 ± 1.3	7.0 ± 1.6	7.1 ± 1.1
f_{CSF}	3.1 ± 1.3***	n.d.	2.3 ± 1.3***	n.d.	8.3 ± 2.5	n.d.
tNAA	7.1 ± 1.7	7.4 ± 0.5	6.5 ± 0.5*	6.0 ± 0.7	7.9 ± 1.5	5.4 ± 1.1††
tCr	7.8 ± 1.6	6.9 ± 1.6	7.2 ± 0.6**	6.6 ± 1.4	9.2 ± 1.6	6.8 ± 1.6††
Cho	2.2 ± 0.5	2.0 ± 0.3	1.8 ± 0.2**	1.8 ± 0.2	2.6 ± 0.7	1.8 ± 0.5†
Ins	6.0 ± 1.2	6.0 ± 1.7	5.2 ± 1.4	6.4 ± 1.3	6.6 ± 1.4	6.0 ± 1.6
Glc	6.2 ± 2.3*	0.8 ± 1.2†††	5.4 ± 2.7*	1.1 ± 0.7††	9.8 ± 3.9	1.7 ± 1.3†††
Lac	1.9 ± 1.4	13.9 ± 4.0†††	1.1 ± 1.0**	15.6 ± 1.9†††	2.8 ± 0.8	14.8 ± 3.4†††

The values represent mean ± SD averaged across animals. FWHM = full width at half maximum in Hz, SNR = signal-to-noise ratio as determined by LCModel, and f_{CSF} = CSF partial volume fraction in percent of VOI (n.d., not determined). Metabolite concentrations are given in mM per liter of VOI after correcting for CSF partial volumes.
*$P < 0.05$, **$P < 0.01$, and ***$P < 0.001$ unpaired *t*-test vs. C57BL/6 mice in vivo
$^{\dagger}P < 0.05$, $^{\dagger\dagger}P < 0.01$, and $^{\dagger\dagger\dagger}P < 0.001$ paired *t*-test of in vivo and post mortem data within mouse strains.

in vivo (3) and in vitro (16,17). Beyond these findings, however, C57BL/6 mice presented with the highest brain concentrations of tNAA, tCr, Cho, and Ins (not significant) of all three strains studied. Based on the fact that tCr emerges as a constituent of all brain cells, the simultaneous occurrence of elevated concentrations of the neuroaxonal marker tNAA and the glial components Cho (mainly oligodendrocytes) and Ins (astrocytes) suggest a higher cell density in the brain of C57BL/6 mice than in other strains. These findings parallel the observation of much larger ventricular spaces than in NMRI and BALB/c mice. Finally, it should be noted that the highest levels of both Glc and Lac found in C57BL/6 mice may indicate strain-dependent differences of the cerebral energy metabolism (see below).

Metabolic Responses to Global Ischemia

Both the post mortem proton MR spectra shown in Fig. 3 and the metabolite concentrations summarized in Table 2 reveal strain-dependent differences of metabolic alterations in response to global irreversible ischemia. Apart from an immediate nonoxidative consumption of Glc, which depletes accessible pools and yields a corresponding prominent accumulation of Lac in all animals, C57BL/6 mice exhibit significant reductions of tNAA, tCr, and Cho in the early post mortem phase, whereas pertinent metabolite levels remained unchanged in NMRI and BALB/c mice until at least 1 hr post mortem.

This finding seems to reflect selective aspects of the reported increased vulnerability of C57BL/6 mice to ischemic insults. Similar reductions of tNAA (25–27) and/or tCr (25) were observed 30–60 min after global ischemia in rats, while no such changes were found in rabbit brain using in vitro proton MRS (28). The rapid loss of tNAA during global ischemia is in line with earlier studies (27,29) suggesting an initially reversible state of neuronal dysfunction prior to cellular degeneration. Here, the reduced metabolite concentrations cannot result from a generalized dilution due to a vasogenic edema (30) because the brain water content does not significantly increase without circulation. Moreover, the onset of substantial neuronal disintegration and subsequent tNAA washout, which has been discussed as the underlying factor in focal ischemia (26), is unlikely to occur in an early post mortem condition. In addition, because the experimental conditions were similar for all strains after cardiac arrest, differential alterations of the brain temperature are also unlikely to cause the more rapid decrease of major metabolites in C57BL/6 mice.

Another possible explanation may be due to strain-related differences in the cerebral energy status and/or glucose transport. For example, the relatively high in vivo concentration of Lac found for the C57BL/6 strain (compare Table 2) may indicate a partial shift of the energy metabolism from oxidative phosphorylation toward enhanced anaerobic glycolysis and therefore cause a more vulnerable condition. On the other hand, the corresponding Glc/Lac concentration ratio of 3.6 ± 1.5 is not significantly different from 3.2 ± 2.8 for NMRI and 3.3 ± 1.4 for BALB/c mice and within the range found in proton MRS studies of rat brain in vivo (14,31,32). However, this observation is based on a Glc concentration which is also abnormally high. It may be the result of increased glucose transport but certainly requires further investigation.

CONCLUSIONS

In summary, the present work underlines the feasibility of localized proton MRS of mouse brain and demonstrates strain-related differences in the basal cerebral metabolite concentrations in vivo as well as in the metabolic responses to irreversible global ischemia. While MRI and proton MRS reveal similar neuroanatomic properties and metabolic characteristics of NMRI and BALB/c mice, the C57BL/6 strain differs from these strains in various respects: 1) C57BL/6 mice exhibit the largest ventricular spaces (and largest proton MRS linewidths); 2) they possess the highest cellular density, as indicated by the highest brain concentrations of tNAA, tCr, Cho, and Ins; 3) they present with putative alterations of the energy metabolism as supported by the highest brain concentrations of Glc and Lac; and 4) they reveal an accelerated neuroaxonal

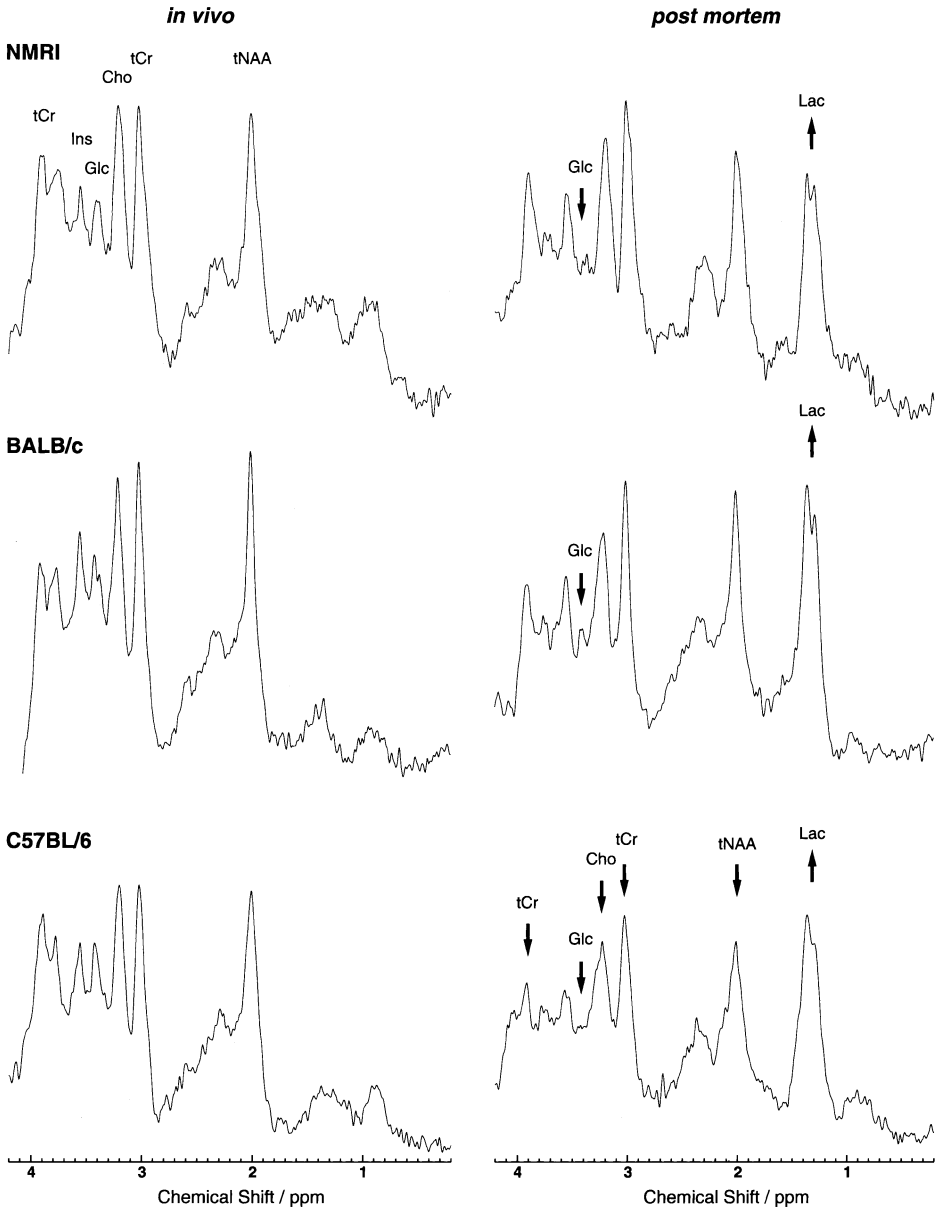

FIG. 3. In vivo (left) and 1 hr post mortem (right) proton MR spectra of the same animal for different mouse strains (STEAM, TR/TE/TM = 6000/20/10 ms, 4 × 3 × 4 mm^3 VOI, corrected for CSF and scaled with respect to brain water content). Metabolite resonances include *N*-acetylaspartate (tNAA), creatine and phosphocreatine (tCr), choline-containing compounds (Cho), *myo*-inositol (Ins), glucose (Glc), and lactate (Lac). Apart from decreased Glc and increased Lac post mortem, the specific vulnerability of the C57BL/6 strain to ischemia is demonstrated by the reduction of tNAA, tCr, and Cho in contrast to NMRI and BALB/c mice.

damage during ischemia as evidenced by an immediate reduction of major metabolite pools post mortem. These findings are in line with the previously reported vulnerability of C57BL/6 mice to ischemia and suggest the relevance of intrinsic metabolic factors.

REFERENCES

1. Huang Z, Huang PL, Panahian N, Dalkara T, Fishman MC, Moskowitz MA. Effects of cerebral ischemia in mice deficient in neuronal nitric oxide synthase. Science 1994;265:1883–1885.
2. Yang G, Chan PH, Chen J, Carlson E, Chen SF, Weinstein P, Epstein CJ, Kamii H. Human copper-zinc superoxide dismutase transgenic mice are highly resistant to reperfusion injury after focal cerebral ischemia. Stroke 1994;25:165–170.
3. in't Zandt HJA, Klomp DWJ, Oerlemans F, van der Zee CEEM, Wieringa B, Heerschap A. Absolute quantitative localized 1H MR spectroscopy and MRI on the in vivo mouse brain: effect of genetic background. In: Proc 8th Annual Meeting ISMRM, Denver, 2000. 8:180.
4. Fujii M, Hara H, Meng W, Vonsattel JP, Huang Z, Moskowitz MA. Strain-related differences in susceptibility to transient forebrain ischemia in SV-129 and C57black/6 mice. Stroke 1997;28:1805–1810.
5. Connolly ES Jr, Winfree CJ, Stern DM, Solomon RA, Pinsky DJ. Procedural and strain-related variables significantly affect outcome in a murine model of focal cerebral ischemia. Neurosurgery 1996;38:523–531.
6. Wellons JC 3rd, Sheng H, Laskowitz DT, Burkhard Mackensen G, Pearlstein RD, Warner DS. A comparison of strain-related susceptibility in two murine recovery models of global cerebral ischemia. Brain Res 2000;868:14–21.
7. Yang G, Kitagawa K, Matsushita K, Mabuchi T, Yagita Y, Yanagihara T, Matsumoto M. C57BL/6 strain is most susceptible to cerebral ischemia following bilateral common carotid occlusion among seven mouse strains: selective neuronal death in the murine transient forebrain ischemia. Brain Res 1997;752:209–218.
8. Majid A, He YY, Gidday JM, Kaplan SS, Gonzales ER, Park TS, Fenstermacher JD, Wei L, Choi DW, Hsu CY. Differences in vulnerability to permanent focal cerebral ischemia among 3 common mouse strains. Stroke 2000;31:2707–2714.

9. Beckmann N. High resolution magnetic resonance angiography noninvasively reveals mouse strain differences in the cerebrovascular anatomy in vivo. Magn Reson Med 2000;44:252–258.
10. Maeda K, Hata R, Hossmann KA. Differences in the cerebrovascular anatomy of C57black/6 and SV129 mice. Neuroreport 1998;9:1317–1319.
11. Barone FC, Knudsen DJ, Nelson AH, Feuerstein GZ, Willette RN. Mouse strain differences in susceptibility to cerebral ischemia are related to cerebral vascular anatomy. J Cereb Blood Flow Metab 1993; 13:683–692.
12. Hata R, Mies G, Wiessner C, Fritze K, Hesselbarth D, Brinker G, Hossmann KA. A reproducible model of middle cerebral artery occlusion in mice: hemodynamic, biochemical, and magnetic resonance imaging. J Cereb Blood Flow Metab 1998;18:367–375.
13. Pouwels PJW, Frahm J. Regional metabolite concentrations in human brain as determined by quantitative localized proton MRS. Magn Reson Med 1998;39:53–60.
14. Michaelis T, Wick M, Fujimori H, Matsumura A, Frahm J. Proton MRS of oral creatine supplementation in rats. Cerebral metabolite concentrations and ischemic challenge. NMR Biomed 1999;12:309–314.
15. Michaelis T, de Biurrun G, Watanabe T, Frahm J, Ohl F, Fuchs E. Gender-specific alterations of cerebral metabolites with aging and cortisol treatment. J Psychiatr Res 2001;35:231–237.
16. Jenkins BG, Klivenyi P, Küstermann E, Andreassen OA, Ferrante RJ, Rosen BR, Beal MF. Nonlinear decrease over time in N-acetyl aspartate levels in the absence of neuronal loss and increases in glutamine and glucose in transgenic Huntington's disease mice. J Neurochem 2000; 74:2108–2119.
17. Tsao JW, Paramananthan N, Parkes HG, Dunn JF. Altered brain metabolism in the C57BL/Wld mouse strain detected by magnetic resonance spectroscopy association with delayed Wallerian degeneration? J Neurol Sci 1999;168:1–12.
18. Gruetter R. Automatic, localized in vivo adjustment of all first- and second-order shim coils. Magn Reson Med 1993;29:804–811.
19. Provencher SW. Estimation of metabolite concentrations from localized in vivo proton NMR spectra. Magn Reson Med 1993;30:672–679.
20. Tracey I, Dunn JF, Parkes HG, Radda GK. An in vivo and in vitro 1H-magnetic resonance spectroscopy study of mdx mouse brain: abnormal development or neural necrosis? J Neurol Sci 1996;141:13–18.
21. Schwarcz A, Berente Z, Osz E, Doczi T. In vivo water quantification in mouse brain at 9.4 Tesla in a vasogenic edema model. Magn Reson Med 2001;46:1246–1249.
22. Kinouchi H, Epstein CJ, Mizui T, Carlson E, Chen SF, Chan PH. Attenuation of focal cerebral ischemic injury in transgenic mice overexpressing CuZn superoxide dismutase. Proc Natl Acad Sci USA 1991;88: 11158–11162.
23. Ernst T, Kreis R, Ross BD. Absolute quantitation of water and metabolites in the human brain. I. Compartments and water. J Magn Reson B 1993;102:1–8.
24. Hesselbarth D, Franke C, Hata R, Brinker G, Hoehn-Berlage M. High resolution MRI and MRS: a feasibility study for the investigation of focal cerebral ischemia in mice. NMR Biomed 1998;11:423–429.
25. Higuchi T, Fernandez EJ, Maudsley AA, Weiner MW. Mapping of cerebral metabolites in rats by 1H magnetic resonance spectroscopic imaging. Distribution of metabolites in normal brain and postmortem changes. NMR Biomed 1993;6:311–317.
26. Sager TN, Laursen H, Hansen AJ. Changes in N-acetyl-aspartate content during focal and global brain ischemia of the rat. J Cereb Blood Flow Metab 1995;15:639–646.
27. Brulatout S, Meric P, Loubinoux I, Borredon J, Correze JL, Roucher P, Gillet B, Berenger G, Beloeil JC, Tiffon B, Mispelter J, Seylaz J. A one-dimensional (proton and phosphorus) and two-dimensional (proton) in vivo NMR spectroscopic study of reversible global cerebral ischemia. J Neurochem 1996;66:2491–2499.
28. Petroff OA, Ogino T, Alger JR. High-resolution proton magnetic resonance spectroscopy of rabbit brain: regional metabolite levels and postmortem changes. J Neurochem 1988;51:163–171.
29. Dautry C, Vaufrey F, Brouillet E, Bizat N, Henry PG, Conde F, Bloch G, Hantraye P. Early N-acetylaspartate depletion is a marker of neuronal dysfunction in rats and primates chronically treated with the mitochondrial toxin 3-nitropropionic acid. J Cereb Blood Flow Metab 2000; 20:789–799.
30. Gyngell ML, Busch E, Schmitz B, Kohno K, Back T, Hoehn-Berlage M, Hossmann KA. Evolution of acute focal cerebral ischaemia in rats observed by localized 1H MRS, diffusion-weighted MRI, and electrophysiological monitoring. NMR Biomed 1995;8:206–214.
31. Nagatomo Y, Wick M, Prielmeier F, Frahm J. Dynamic monitoring of cerebral metabolites during and after transient global ischemia in rats by quantitative proton NMR spectroscopy in vivo. NMR Biomed 1995; 8:265–270.
32. Pfeuffer J, Tkac I, Provencher SW, Gruetter R. Toward an in vivo neurochemical profile: quantification of 18 metabolites in short-echo-time 1H NMR spectra of the rat brain. J Magn Reson 1999;141:104–120.